

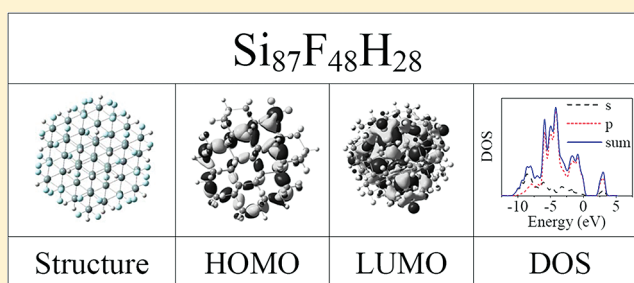
Theoretical Study of the Electronic Properties of Silicon Nanocrystals Partially Passivated with Cl and F

Estrella Ramos, B. Marel Monroy,* Juan Carlos Alonso, Luis E. Sansores, Roberto Salcedo, and Ana Martínez

Instituto de Investigaciones en Materiales, Universidad Nacional Autónoma de México, Circuito Exterior S. N., Ciudad Universitaria, CP 04510, México D.F.

Supporting Information

ABSTRACT: Density functional theory calculations and theoretical representations of the density of states (DOS) were undertaken in order to understand the electronic properties of silicon nanocrystals (Si-nc), when partially passivated with Cl and F. Effects relating to cluster size (Si_{29} , Si_{35} , and Si_{87}), type, and percentages of halogen surface passivant, concerning both the cluster gap and electron-donor–acceptor capabilities, were analyzed. These calculations indicate that as the percentage of Cl and F substitution increases, the energy of the LUMO decreases, and consequently, the HOMO–LUMO gap decreases. Correspondingly, we found that the high-electronegativity substituent Cl and F atoms produce the appearance of shoulders in the DOS band edges, thus reducing the band gap. These results explain the photoluminescent experimental data reported for Si-nc. The evaluation of the electrodonating and electroaccepting powers of Si-nc partially passivated with Cl and F indicates that Si-nc have potential applications for bulk heterojunction solar cells and electroluminescent devices.



INTRODUCTION

The investigation of silicon nanocrystals (Si-nc) embedded in thin films of a variety of silicon compounds such as silicon oxide (SiO_2),^{1–7} hydrogenated silicon nitride ($\text{SiN}_x\text{:H}$),^{8–14} chlorinated silicon nitride ($\text{SiN}_x\text{:Cl}$),^{14–19} hydrogenated polymorphous silicon (pm-Si:H),^{20,21} and hydrogenated polymorphous silicon carbon ($\text{pm-Si}_{1-x}\text{C}_x\text{:H}$)²² has attracted increasing interest motivated by their luminescent, optical, and electronic properties which may be expedient for optoelectronic and photonic applications. Although there is consensus that the quantum confinement effect (QCE) in the Si-nc plays a crucial role in determining their optoelectronic properties, many of these experimental results show that passivation of Si-nc and the chemical environment of the surrounding matrix may significantly influence the structural stability and optoelectronic properties of these nanocrystals.^{1–3,7–12,14,15,17–22}

The electronic and optical properties of Si-nc have also been investigated theoretically, using different methods and approximations. Most of the theoretical calculations of the electronic structure of Si-nc have been performed on hydrogen-passivated Si-nc, and these have indicated that the HOMO–LUMO gap, i.e., the energy difference between the HOMO (highest occupied molecular orbital) and the LUMO (lowest unoccupied molecular orbital) increases, as the size of the Si-nc decreases, in conformity with the QCE.^{9,10,23–33} Some of these theoretical reports indicate that a gap reduction of more than 1 eV arises in fully hydrogenated-small Si-nc ($\text{Si}_{35}\text{H}_{36}$)

when two hydrogen atoms are replaced by double-bonded oxygen (O) or sulfur (S), or a single hydrogen atom is replaced by single-bonded CH_2 or a single bridged-nitrogen atom (to form $\text{Si}_{35}\text{H}_{34}\text{O}$, $\text{Si}_{35}\text{H}_{34}\text{S}$, $\text{Si}_{35}\text{H}_{34}\text{CH}_2$, or $\text{Si}_{35}\text{H}_{34}\text{NH}$ nanoclusters, respectively).^{9,10,27,29,30} Other interesting results derived from theoretical analysis indicate that the substitution of a single surface hydrogen atom by a single electronegative passivant such as chlorine or fluorine (to form $\text{Si}_{35}\text{H}_{34}\text{Cl}$ or $\text{Si}_{35}\text{H}_{34}\text{F}$, respectively) has little effect on the Si-nc gap (with a reduction of only 0.1–0.2 eV).^{29,30} The reduction of the gap is also minimal (~ 0.1 eV) when a single hydrogen atom at the surface of the Si-nc is replaced by OH to form $\text{Si}_{35}\text{H}_{34}\text{OH}$. However, when the Si-nc surface is completely passivated with OH, to form $\text{Si}_{35}(\text{OH})_{36}$, the gap becomes considerably smaller (by ~ 2.3 eV).³¹

Motivated by these studies and considering the fact that the use of halogen-containing gases has become attractive for the preparation of silicon nanocrystals with stable luminescent and electronic properties,^{14,16,19} in a previous work we reported the HOMO–LUMO gap of Si-nc, when the surface was completely passivated with chlorine and nitrogen. We found that the gaps for $\text{Si}_{35}\text{Cl}_{36}$ (3.3 eV) and $\text{Si}_{35}(\text{NH}_2)_{36}$ (3.2 eV) were significantly smaller than the gap for $\text{Si}_{35}\text{H}_{36}$ (5.1 eV).³⁴ We also discovered that the charge transfer capacity of Si-nc where

Received: December 13, 2011

Revised: January 16, 2012

Published: January 17, 2012

the surface was completely passivated with chlorine or nitrogen became modified in opposite directions with respect to hydrogen passivated Si-nc, acting as good electron acceptors when Cl atoms are present and good electron donors when NH_2 passivation occurs.³⁴ All of the previously presented calculations provided valuable information for understanding the effect of surface passivation or surface chemistry, on the electronic and optical properties of Si-nc.

In order to evolve an improved model for the experimental results that are obtained under different experimental conditions,^{2,15,16,35} it is important to use different passivants (for example H, Cl, F, or N) and likewise vary the amounts of substitution. In a recent theoretical study, the HOMO–LUMO gap for Si-nc with different percentages of surface Cl coverage (ranging from one Cl atom up to 25, 50, 89, or 100% of Cl) was calculated,³⁶ in order to study the electronic and optical properties of Cl- incorporated on Si-nc, taking into account possible variations in experimental conditions. In spite of these results, there are no theoretical studies for systems with F as substituent and neither are there for the analysis of the electron donor–acceptor capacity of these clusters, either with or without halogen substitution. For this reason, in this work we present the HOMO–LUMO gap and the results of the charge transfer capacity of Si-nc passivated with different percentages of chlorine (Cl) and fluorine (F), using a method indicating values for HOMO–LUMO gaps which correlates quite well with the experimental results measured by photoluminescence and electroluminescence.³⁴ As the evaluation of the charge transfer capacity is important for the design of bulk heterojunction solar cells³⁷ and electroluminescent devices,¹⁹ we also calculated properties, such as the electrodonating and electroaccepting powers of Si-nc when they were partially passivated with Cl and F. In order to obtain information about the influence of the electronegativity of the substituent atom on the specific form of the band edges (occupied and unoccupied states), the theoretical representations of the density of states (DOS) are presented for the systems studied in this investigation. These results are directly related to the optical and electronic transitions of these systems, and potential applications in photovoltaic devices are also discussed.

THEORETICAL CALCULATIONS

Density functional approximation^{38–40} as implemented in *Gaussian 09*⁴¹ was used in all calculations. Full geometry optimizations without symmetry constraints were obtained, with the three parameter hybrid functional within the density functional theory (DFT) framework,⁴² applying Perdew and Wang's 1991 gradient-corrected correlation functional⁴³ (B3PW91) and the 6-31G(d,p) basis set.⁴⁴ The starting point consisted of three different size clusters (Si_{29} , Si_{35} , and Si_{87}) which were constructed maintaining the crystalline silicon structural behavior. The symmetry was maintained as T_d and 6-member boat type rings. Consequently, at the surface we only had Si–H and Si– H_2 terminations which changed with the size of the cluster. Different initial geometries were used for the geometry optimization, taking into account that there are two possible replacements for the H atoms: coming from the terminal silicon atoms that are bonded to a single hydrogen atom (Si–H) or coming from the silicon atoms that are bonded to two H atoms (Si– H_2). This study was carried out considering both possibilities; namely Si–L, Si– L_2 , and also L–Si–H ($L = \text{F}$ or Cl). In all cases, symmetry was maintained. Following optimization, it was apparent that the substituted

structures were slightly distorted, when compared to the corresponding structures with hydrogen atoms. Other structures with random substitution of the H atoms were also calculated, but the resulting structures were less stable due to loss of symmetry. The Connolly surface was used to estimate the size of the Si-nc.⁴⁵ Vertical ionization energy (I) and vertical electron affinity (A) were assessed, using single point energy calculations for the cation and the anion, with the optimized structure of the corresponding neutrals.

The Density of States (DOS) for all systems being studied was obtained in the framework of DFT-GGA, utilizing the PW91 exchange and correlation functional. The core electrons were described using ultrasoft Vanderbilt pseudopotentials⁴⁶ within the CASTEP code,^{47,48} as implemented in the Materials Studio software suite. The kinetic energy cutoff for the plane-wave basis set was 300 eV. The Brillouin zone was sampled with a highly converged set of k points in accordance with the Monkhorst Pack scheme.⁴⁹ The cluster geometry corresponds to the optimized Gaussian structure described above. Clusters were then placed in a cubic simulation cell with periodic boundary conditions. The size of the simulation cell was chosen so that the distance between the cluster and its replica (due to the periodic boundary conditions) exceeded 10 Å. Taking this into account, interactions between the clusters and their replicas are negligible.

RESULTS AND DISCUSSION

Structural Results. Three main issues are analyzed in this paper which may influence the HOMO–LUMO gap and the electron donor–acceptor capabilities: the size of the cluster (Si_{29} , Si_{35} and Si_{87}), the substituent atom (F and Cl) and the percentage of substitution (0%, 32–37%, 63–67%, 100%). The amount of substitution on the Si-nc and the corresponding chemical formulas are presented in Table 1. L represents F or Cl and x is the percentage of substitution of the H atoms at the surface.

Table 1. Percentages of Substitution on the Si-nc and the Corresponding Chemical Formulas Are Presented, where L is F or Cl

$x = 0\%$	$\text{Si}_{29}\text{H}_{36}$	$\text{Si}_{35}\text{H}_{36}$	$\text{Si}_{87}\text{H}_{76}$
$x = 32\text{--}37\%$	$\text{Si}_{29}\text{L}_{12}\text{H}_{24}$	$\text{Si}_{35}\text{L}_{12}\text{H}_{24}$	$\text{Si}_{87}\text{L}_{28}\text{H}_{48}$
$x = 63\text{--}67\%$	$\text{Si}_{29}\text{L}_{24}\text{H}_{12}$	$\text{Si}_{35}\text{L}_{24}\text{H}_{12}$	$\text{Si}_{87}\text{L}_{48}\text{H}_{28}$
$x = 100\%$	$\text{Si}_{29}\text{L}_{36}$	$\text{Si}_{35}\text{L}_{36}$	$\text{Si}_{87}\text{L}_{76}$

All structures were fully optimized starting from different initial geometries. The calculated diameters of the resulting Si-nc are 1.17, 1.22, and 1.66 nm for fully hydrogenated Si_{29} , Si_{35} and Si_{87} , respectively. This diameter increases when H atoms are substituted by F or Cl due to the larger size of the halogen atoms in comparison with the H atom. For systems where 100% substitution takes place, the diameter increases by 0.07 and 0.22 nm, when the substituent is F or Cl respectively. It is worth mentioning that the sizes of these Si-nc correspond to the lowest possible limit which can be obtained experimentally.^{8,17} In Figure 1, the optimized structure for $\text{Si}_{87}\text{H}_{76}$ is presented as an example. It shows T_d symmetry with the terminal silicon atoms bonded to either one or two hydrogen atoms. Similar structures were constructed for the other clusters and coordinates are reported as Supporting Information.

HOMO–LUMO Gap and the Density of States (DOS). It is possible to analyze the size and the substituent effects on the

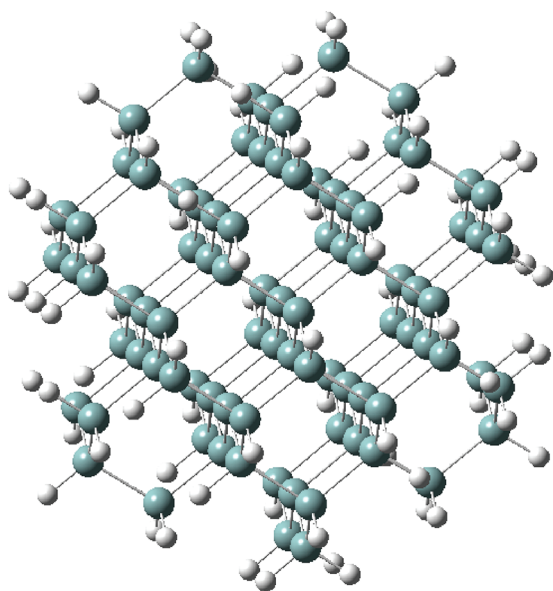


Figure 1. Optimized structure of $\text{Si}_{87}\text{H}_{76}$ (B3PW91/6-31G(d,p)) is presented.

HOMO–LUMO gap, taking the results reported in Figure 2. Predictably, as a result of the QCE for completely hydro-

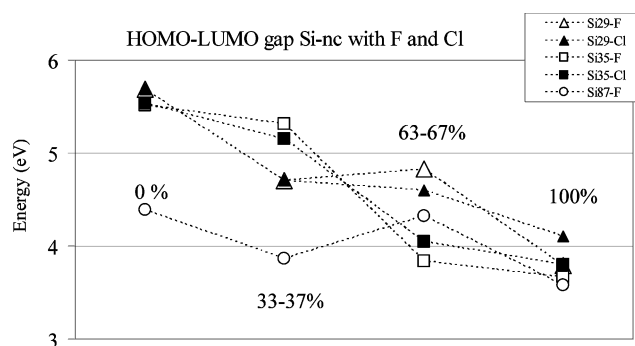


Figure 2. HOMO–LUMO gaps for all optimized structures with partial substitution of superficial H atoms ranging between 0% and 100% are presented.

genated systems ($x = 0\%$), the HOMO–LUMO gap decreases, as the size of the Si-nc increases. This effect disappears gradually as the percentage of substitutions increases. From these results, it is possible to conclude that when H atoms are totally replaced by F or Cl, the influence of the substitution on the HOMO–LUMO gap is stronger than the effect of the size of the system, and apparently the QCE is masked. In order to have the smallest HOMO–LUMO gap for opto-electronic applications in the visible spectral range, the optimal percentage

of substitution for Si_{87} is 33–37% and 100%. For Si_{35} and Si_{29} , the most favorable substitution for producing the smallest HOMO–LUMO gap is 100%. It is noteworthy that our gap calculations correlate quite well with experimental data. For instance, optical absorption gaps of around 4 eV have been measured from transmittance spectra in silicon nitride thin films containing Si-nc, partially passivated with Cl and likewise photoluminescence peaks of around 3.2 eV have been identified, associated with Si-nc with diameters measuring around 1 nm.¹⁷

In order to have insight concerning the effects responsible for the decline in the HOMO–LUMO gap, we analyzed the corresponding eigenvalues and the DOS for all clusters. The eigenvalues of the HOMO and the LUMO are presented in Table 2. These values correlate with the percentage of substitution. Generally, as the amount of F and Cl increases, the eigenvalues decrease. The only exception is in the case of the LUMO value for $\text{Si}_{87}\text{F}_{48}\text{H}_{28}$. All systems present the lowest eigenvalues in the instance when total substitution is implemented (100%). The presence of F or Cl modifies the energy of the LUMO more than it does the energy of the HOMO. More than 2 eV of difference exists between the LUMO values of Si-nc passivated with hydrogen atoms and Si-nc passivated with F or Cl, whereas the difference in the HOMO values is close to 1 eV. This means that the electron affinity for the substituted cluster is increasing along with the percentage of substitution, whereas the ionization energy remains more or less constant. This is a logical finding due to the high electron affinity of F and Cl when compared to the electron affinity of the H atom. These results also indicate that the main reason for the reduction in the HOMO–LUMO gap is the decrease in the energy pertaining to the LUMO.

Figure 3 presents the HOMO–LUMO orbitals and the density of states (DOS) of Si_{87} , with different percentages of substitution. All the molecular orbitals presented in this figure represent bonding orbitals between silicon atoms. The shape of the LUMO orbital is quite similar for all the systems shown in the figure. The principal difference is found in the case of the HOMO orbital, which is situated inside the cluster if there are no F atoms present and at the surface of the cluster if all the H atoms are substituted by F atoms. This means that an excited electron will go from an external molecular orbital (HOMO) to an internal molecular orbital (LUMO). Since both HOMO and LUMO are Si–Si bonding orbitals, no modifications in the geometry are expected from the excitation. The major difference will concern electron density. In the case of the fully hydrogenated cluster, the electron transfer occurs in the same region as both, HOMO and LUMO, are within the cluster. Contrastingly, for clusters with F passivation, the electronic transfer occurs from the orbitals at the surface of the cluster (HOMO) to the orbitals within the cluster (LUMO).

Table 2. Eigenvalues of the HOMO and the LUMO (eV)

Si_{87}	HOMO	LUMO	Si_{35}	HOMO	LUMO	Si_{29}	HOMO	LUMO
H_{76}	−6.2	−2.3	H_{36}	−6.8	−1.7	H_{36}	−6.9	−1.7
$\text{F}_{28}\text{H}_{48}$	−7.1	−3.7	$\text{F}_{12}\text{H}_{24}$	−7.1	−2.3	$\text{F}_{12}\text{H}_{24}$	−7.3	−3.1
$\text{F}_{48}\text{H}_{28}$	−7.2	−3.4	$\text{F}_{24}\text{H}_{12}$	−7.6	−4.2	$\text{F}_{24}\text{H}_{12}$	−7.6	−3.3
F_{76}	−7.9	−4.8	F_{36}	−8.0	−4.8	F_{36}	−7.8	−4.5
			$\text{Cl}_{12}\text{H}_{24}$	−7.3	−2.6	$\text{Cl}_{12}\text{H}_{24}$	−7.4	−3.1
			$\text{Cl}_{24}\text{H}_{12}$	−7.6	−4.0	$\text{Cl}_{24}\text{H}_{12}$	−7.6	−3.6
			Cl_{36}	−7.7	−4.4	Cl_{36}	−7.8	−4.2

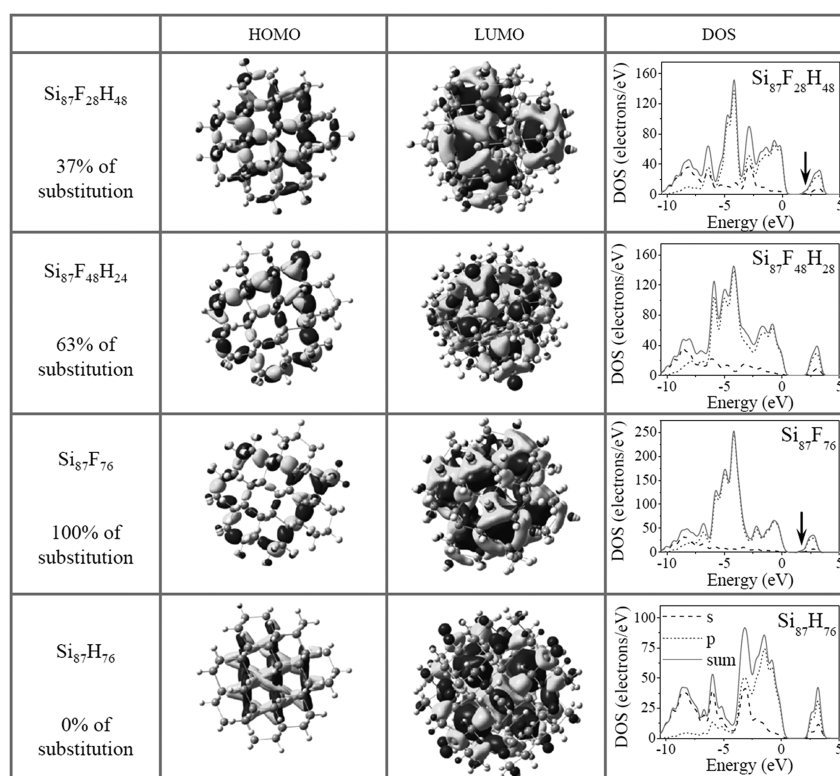


Figure 3. HOMO and LUMO orbitals and DOS of Si_{87} -nc with different percents of F substitution. The appearance of shoulders in the band edges of the DOS is indicated by arrows.

Clusters with halogen substitution will show a modification in terms of electron density for the HOMO–LUMO electronic transitions which is an important difference when compared to systems with H. The experimental consequences of this fact may be associated with different radiative recombination probabilities (generally associated with HOMO–LUMO electronic transitions) and thus different recombination lifetimes in fully or partially halogenated clusters with respect to fully hydrogenated ones. Evidently, this may represent an important area, requiring further study.¹⁰

The differences in electron density as a function of the percentage of F substitution can be better understood with the DOS representation displayed in Figure 3. The valence band is shifted to lower energy values as the halogen concentration increases as a consequence of the halogen's electronegativity. This is evident in two aspects: (i) the deformation of the band edges resulting in the appearance of shoulders that reduce the band gap and (ii) the appearance of intense peaks around -5 eV corresponding to the p orbitals of the halogen. These peaks increase in intensity with increasing halogen substitution (note the scales in the DOS graphs in Figure 3). The deformation of the band edges corresponds with the observed trends of the HOMO–LUMO gap reported in Figure 2, and the LUMO eigenvalues displayed in Table 2. The fully hydrogenated cluster has sharp band edges and its gap is larger than the gaps of the clusters with different percentages of F substitution. For the cluster with 37% of substitution and the fully substituted cluster, a shoulder appears in the unoccupied states region (indicated by the arrows in Figure 3). This result correlates quite well with the observed decrease in the HOMO–LUMO gaps reported in Figure 2. Si_{87} with 63% of substitution displays sharp band edges, increasing the gap for this cluster. To explain this trend, it is important to notice that when the percentage of

passivation is 37%, the F substitution was carried out for silicon atoms which were bonded to a single H atom. Contrastingly, in order to obtain 63% of passivation, substitution was undertaken for silicon atoms that were bonded to two H atoms. The asymmetry of the charge distribution of the silicon atoms at the surface is responsible for the appearance of the shoulder in the unoccupied states of the DOS. This asymmetry is more pronounced where there is only one F substitution, than when there are two F substitutions in the same Si atom at the surface. The same trend was observed for all of the systems studied in this work.

In order to analyze the effect of electronegativity on the shape of the DOS, Figure 4 illustrates the case of the Si_{35} cluster, passivated with F, Cl, and H, respectively. There is a small shoulder indicated by an arrow which is induced by the presence of F or Cl. This deformation of the band edges is responsible for the smaller gap observed for all the fully halogenated clusters, regardless of their size. Also, in this case there is a pronounced peak in the DOS when F or Cl is present. This peak is more intense and appears at lower energies in the case of the more electronegative passivant (F). From these observations, it is possible to infer that the effect of the electronegativity of the substituent is to shift the electronic states to lower energies. This produces a deformation of the band edges that will influence the optical and electronic properties of these systems. This phenomenon is similar to the effect of doping and/or stress, which have both been observed to similarly deform the DOS in theoretical calculations and experimental measurements, as well.^{50–52}

Electron Donor–Acceptor Properties: Photovoltaic Cells. The simplest photovoltaic device is based on a bulk-heterojunction architecture of two semiconductor compounds: one is “n” type (an electron donor) and the other one is “p”

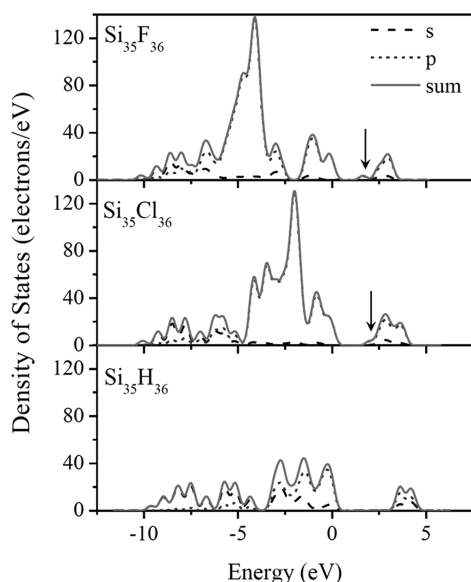


Figure 4. DOS of Si₃₅-nc passivated with F, Cl, and H, respectively. The effect of the electronegativity of the halogen passivation is evident in the shoulder that appears in the band edges (indicated by the arrows).

type (an electron acceptor). The photovoltaic process begins with light absorption and ends with charge transport to the electrodes. In terms of the absorption of light, the value of the HOMO–LUMO gap is crucial. In order to have photovoltaic materials for the construction of solar cells, the HOMO–LUMO gap of the electron donor has to be around 2 eV as this corresponds to the maximum in the solar radiation energy spectrum. Also, it is well-known that in order to facilitate the charge transport to the electrodes in a solar cell, it is necessary to have an electron donor with low ionization energy and an electron acceptor with high electron affinity.

A useful way of measuring electrodonating and electro-accepting powers has recently been described by Gázquez et al.⁵² They established a simple charge-transfer model and analyzed the global response of a molecule immersed in an idealized environment that may either withdraw or donate charge. An alternative quadratic interpolation for the energy as a function of the number of electrons was proposed, in order to evaluate the response of a molecule to charge acceptance or withdrawal, in terms of its electron affinity and ionization potential. Referring to this approximation, these authors conclude that the propensity to donate charge, or electro-donating power may be defined as

$$\omega^- = \frac{(3I + A)^2}{16(I - A)} \quad (1)$$

whereas, the propensity to accept charge, or electroaccepting power, may be defined as

$$\omega^+ = \frac{(I + 3A)^2}{16(I - A)} \quad (2)$$

In the case of electrodonating power, lower values imply a greater capacity for donating charge. In the case of electro-accepting power, higher values imply a greater capacity for accepting charge. The electrodonating and electroaccepting powers are based on a simple charge transfer model, expressed in terms of chemical potential and hardness. Chemical potential

measures the charge flow direction, together with the capacity to donate or accept charge, assigning more emphasis to ionization potential than to electron affinity in the context of the charge donation process. Contrarily, electroaccepting power assigns more significance to electron affinity than to ionization potential. Hardness assesses resistance to the electron flow.

Hardness is defined as the energy difference between *I* and *A*. Following Koopmans's theorem, *I* and *A* are approximated with the absolute value of the energy of the HOMO and the absolute value of the LUMO, respectively. In this approximation, hardness represents the HOMO–LUMO gap. As the HOMO–LUMO gap is important in the design of photovoltaic cells, thus hardness is also important for this application. Following these ideas, it is possible to contemplate ω^- and ω^+ as good indexes for evaluating materials in terms of their capacity as either electron donors or acceptors, and also for correlating these values with their photovoltaic cell performance. Table 3 reports *I* and *A* for all systems being studied. In

Table 3. Ionization Energy (*I*) and Electron Affinity (*A*) Reported in eV

Si ₈₇	<i>I</i>	<i>A</i>	Si ₃₅	<i>I</i>	<i>A</i>	Si ₂₉	<i>I</i>	<i>A</i>
H ₇₆	6.9	1.6	H ₃₆	7.7	0.8	H ₃₆	7.9	0.7
F ₂₈ H ₄₈	7.8	3.0	F ₁₂ H ₂₄	8.1	1.4	F ₁₂ H ₂₄	9.0	1.5
F ₄₈ H ₂₈	8.0	2.6	F ₂₄ H ₁₂	8.6	3.3	F ₂₄ H ₁₂	8.6	2.3
F ₇₆	8.6	4.1	F ₃₆	9.0	3.9	F ₃₆	8.9	3.6
			Cl ₁₂ H ₂₄	8.2	1.8	Cl ₁₂ H ₂₄	8.3	3.6
			Cl ₂₄ H ₁₂	8.4	3.2	Cl ₂₄ H ₁₂	8.5	3.6
			Cl ₃₆	8.6	3.6	Cl ₃₆	8.6	3.4

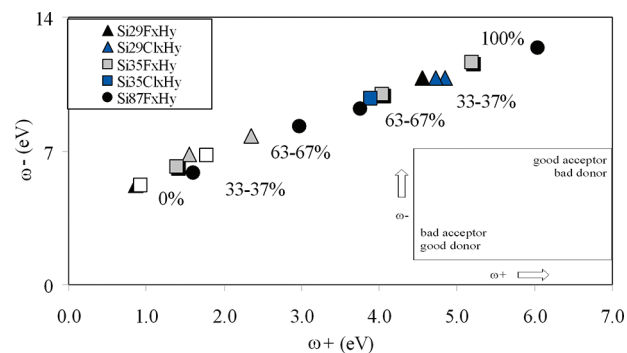


Figure 5. Electron acceptor power (ω^+) and electron donor power (ω^-) are presented.

Figure 5, we include ω^- and ω^+ in order to facilitate the analysis. These values indicate that both size and substituent have an effect on the capacity of Si-nc to either accept or donate charge. The electron affinity increases as the size of the system augments, and systems without H atoms (100% of substitution) have more or less the same ionization energies and similar electron affinities. These systems represent the best electron acceptors and the worse electron donors, as can be expected due to the high electron affinity of F and Cl. On the other hand, systems with 0% of substitution represent better electron donors and worse electron acceptors than systems with F or Cl, and the largest system (Si₈₇) constitutes the best electron donor and the best electron acceptor. This is in agreement with HOMO and LUMO values, given that Si₈₇ presents the highest HOMO and the lowest LUMO. Generally,

the clusters become better electron acceptors and worse electron donors as the percentage of substitution increases. The only exception is $\text{Si}_8\text{F}_{28}\text{H}_{48}$. This system represents a better electron acceptor and better electron donor than $\text{Si}_8\text{F}_{48}\text{H}_{28}$ which possibly relates to the asymmetry in the charge distribution of the Si atoms on the surface when substituting either one or two hydrogen atoms, as was discussed before. Similar results were found and are reported in Figure 5 concerning electrodonating and electroaccepting powers and these are useful for determining whether the system will act as a donor or as an acceptor. As indicated in the same figure, systems located at the top right are good electron acceptors and bad electron donors, and those situated at the bottom left are good electron donors and bad electron acceptors.

For Si-nc substituted 100% with F or Cl, the most probable interaction will be with an electron donor as these are good electron acceptors ("p" type if we use the terms commonly applied to semiconductors). Contrarily, systems with no substitution are good electron donors ("n" type in semiconductors) and they will interact with good electron acceptors. Therefore, if we have Si-nc with different passivations, they would probably act as "p" or "n" semiconductors, depending on the percentage and type of substitution. This analysis indicates that arrays of Si-nc with different passivations may provide building blocks for opto-electronic devices of the p-n junction type, for example photovoltaic cells or electroluminescent devices.^{19,54}

Si-nc systems are good candidates for applications in photovoltaic cells since the HOMO-LUMO gap can be tuned to the size of the system. This can be used in tandem solar cells where the absorption of light is more efficient than in conventional photovoltaic devices.⁵⁴ From the results obtained in this investigation, it can be concluded that the type of passivation plays an important role, both in terms of the absorption of light, as well as concerning the electron-donor-acceptor capabilities of the system. Light absorption is affected by the deformation of the DOS band edges, due to the presence of halogens at the surface. Consequently, the gap reduction caused by surface passivation has to be taken into account, along with QCE. Moreover, the electroaccepting and electrodonating powers of the system are also influenced by the presence of halogens. In order to improve electron affinity, passivation with F or Cl is crucial, as these systems have the highest capacity for accepting electrons and may represent a "p" type material. Completely hydrogenated systems would fulfill the role of "n" type materials needed to form the heterojunction that is required for photovoltaic devices.

CONCLUSIONS

The electronic properties of silicon clusters were explored as a function of three different material properties: the size of the cluster; the substitution of superficial hydrogen atoms by more electronegative atoms (F or Cl); and the percentage of substitution (0%, 32–37%, 63–67%, and 100%). The HOMO-LUMO gap decreased with increasing cluster size, as predicted by QCE for fully hydrogenated clusters. Contrastingly, in the case of fully halogenated Si-nc, the QCE is masked and the HOMO-LUMO gaps have similar values even when the cluster size varies. Analyzing the HOMO-LUMO eigenvalues and calculating the DOS of the systems made it evident that the LUMO is shifted to lower energy values due to the electronegativity of the substituents and that this is reinforced by the appearance of a shoulder at the band

edges of the DOS. Moreover, the occupied states of the DOS are also shifted to lower energies. This shift increases with the percentage of substitution and the electronegativity of the substituent. It was also found that the shoulder of the band edges was related to the asymmetry of the charge distribution on the surface silicon atom, caused by halogen substitution. On the other hand, the analysis of the HOMO and LUMO molecular orbitals exhibits another important difference between fully hydrogenated clusters and substituted clusters. In the first case, both the HOMO and the LUMO are situated inside of the cluster whereas in the latter case, the HOMO is situated at the surface of the cluster and the LUMO is inside. This may have different implications in terms of the HOMO-LUMO transition dynamics for fully hydrogenated systems, as compared with substituted ones. Finally, the electrodonating and electroaccepting powers make it possible to classify the differently passivated systems as either electron donors or electron acceptors. This has important applications for the charge transport process of devices from these materials, in particular, p-n junctions or photovoltaic cells.

ASSOCIATED CONTENT

Supporting Information

The coordinates of all of the constructed structures. This material is available free of charge via the Internet at <http://pubs.acs.org>.

AUTHOR INFORMATION

Corresponding Author

*E-mail: marel@iim.unam.mx.

Notes

The authors declare no competing financial interest.

ACKNOWLEDGMENTS

This study was made possible due to funding from the Consejo Nacional de Ciencia y Tecnología (CONACyT), as well as resources provided by the Instituto de Investigaciones en Materiales IIM, UNAM and support from DGAPA-IACOD through Grant IA101511. The work was carried out, using a KanBalam supercomputer, provided by DGTIC, UNAM. The authors acknowledge Oralia L. Jiménez A, María Teresa Vázquez, Caín González, and Joaquín Morales for their technical support.

REFERENCES

- (1) Cao, Z. X.; Song, R.; Ma, L. B.; Du, Y.; Ji, A. L.; Wang, Y. Q. *Nanotechnology* **2006**, *17*, 2073–2077.
- (2) Nozaki, T.; Sasaki, K.; Ogino, T.; Asahi, D.; Okazaki, K. *Nanotechnology* **2007**, *18*, 235603.
- (3) Godefroo, S.; Hayne, M.; Jivanescu, M.; Stesmans, A.; Zacharias, M.; Lebedev, O. I.; Van Tendeloo, G.; Moshchalkov, V. *Nat. Nanotechnol.* **2008**, *3*, 174–178.
- (4) Marconi, A.; Anopchenko, A.; Wang, M.; Pucker, G.; Bellutti, P.; Pavesi, L. *Appl. Phys. Lett.* **2009**, *94*, 221110.
- (5) Das, D.; Samanta, A. *Nanotechnology* **2011**, *22*, 055601.
- (6) Wang, M.; Anopchenko, A.; Marconi, A.; Moser, E.; Prezioso, S.; Pavesi, L.; Pucker, G.; Bellutti, P.; Vanzetti, L. *Physica E* **2009**, *41*, 912–915.
- (7) Barbagiovanni, E. G.; Goncharova, L. V.; Simpson, P. J. *Phys. Rev. B* **2011**, *83*, 035112.
- (8) Kim, T. W.; Cho, C. H.; Kim, B. H.; Park, S. J. *Appl. Phys. Lett.* **2006**, *88*, 123102.

- (9) Dal Negro, L.; Yi, J. H.; Michel, J.; Kimerling, L. C.; Hamel, S.; Williamson, A.; Galli, G. *IEEE J. Sel. Top. Quant.* **2006**, *12*, 1628–1635.
- (10) Dal Negro, L.; Yi, J. H.; Kimerling, L. C.; Hamel, S.; Williamson, A.; Galli, G. *Appl. Phys. Lett.* **2006**, *88*, 183103.
- (11) Zerga, A.; Carrada, M.; Amann, M.; Slaoui, A. *Physica E* **2007**, *38*, 21–26.
- (12) Hao, H. L.; Wu, L. K.; Shen, W. Z. *Appl. Phys. Lett.* **2008**, *92*, 121922 (3 pages).
- (13) Korchagina, T. T.; Volodin, V. A.; Chichkov, B. N. *Semiconductors* **2010**, *44*, 1611–1616.
- (14) Alonso, J. C.; Santana, G.; Benami, A.; Monroy, B. M. *Encyclopedia Nanosci. Nanotechnol.* **2011**, *16*, 1–31.
- (15) Santana, G.; Monroy, B. M.; Ortiz, A.; Huerta, L.; Alonso, J. C.; Fandiño, J.; Aguilar-Hernández, J.; Hoyos, E.; Cruz-Gandarilla, F.; Contreras-Puentes, G. *Appl. Phys. Lett.* **2006**, *88*, 041916.
- (16) Benami, A.; Santana, G.; Monroy, B. M.; Ortiz, A.; Alonso, J. C.; Fandiño, J.; Aguilar-Hernández, J.; Contreras-Puente, G. *Physica E* **2007**, *38*, 148–151.
- (17) Benami, A.; Santana, G.; Ortiz, A.; Ponce, A.; Romeu, D.; Aguilar-Hernández, J.; Contreras-Puente, G.; Alonso, J. C. *Nanotechnology* **2007**, *18*, 155704.
- (18) López-Suárez, A.; Fandiño, J.; Monroy, B. M.; Santana, G.; Alonso, J. C. *Physica E* **2008**, *40*, 3141–3146.
- (19) Alonso, J. C.; Pulgarín, F. A.; Monroy, B. M.; Benami, A.; Bizarro, M.; Ortiz, A. *Thin Solid Films* **2010**, *518*, 3891–3893.
- (20) Zhang, S.; Liao, X.; Xu, Y.; Martins, R.; Fortunato, E.; Kong, G. *J. Non-Cryst. Solids* **2004**, *338*, 188–191.
- (21) Martins, R.; Raniero, L.; Pereira, L.; Costa, D.; Águas, H.; Pereira, S.; Silva, L.; Gonçalves, A.; Ferreira, I.; Fortunato, E. *Philos. Mag.* **2009**, *89*, 2699–2721.
- (22) Wang, J.; Suendo, V.; Abramov, A.; Yu, L.; Roca i Cabarrocas, P. *Appl. Phys. Lett.* **2010**, *97*, 221113.
- (23) Allan, G.; Delerue, C.; Lannoo, M. *Phys. Rev. Lett.* **1997**, *78*, 3161–3164.
- (24) Ögüt, S.; Chelikowsky, J. R. *Phys. Rev. Lett.* **1997**, *79*, 1770–1773.
- (25) Rohlfing, M.; Louie, S. G. *Phys. Rev. Lett.* **1998**, *80*, 3320–3323.
- (26) Vasiliev, I.; Ögüt, S.; Chelikowsky, J. R. *Phys. Rev. Lett.* **2001**, *86*, 1813–1816.
- (27) Wolkin, M. V.; Jorne, J.; Fauchet, P. M. *Phys. Rev. Lett.* **1999**, *82*, 197–200.
- (28) Vasiliev, I.; Chelikowsky, J. R.; Martin, R. M. *Phys. Rev. B* **2012**, *65*, 121302.
- (29) Puzder, A.; Williamson, A. J.; Grossman, J. C.; Galli, G. *Phys. Rev. Lett.* **2002**, *88*, 097401.
- (30) Puzder, A.; Williamson, A. J.; Grossman, J. C.; Galli, G. *Mater. Sci. Eng., B* **2002**, *96*, 80–85.
- (31) Zhou, Z.; Brus, L.; Friesnet, R. *Nano Lett.* **2003**, *3*, 163–167.
- (32) Hyeon-Deuk, K.; Madrid, A. B.; Prezhdo, O. V. *Dalton Trans.* **2009**, *45*, 10069–10077.
- (33) Madrid, A. B.; Hyeon-Deuk, K.; Habenicht, B. F.; Prezhdo, O. V. *ACS Nano* **2009**, *3*, 2487–2494.
- (34) Martínez, A.; Alonso, J. C.; Sansores, L. E.; Salcedo, R. *J. Phys. Chem. C* **2010**, *114*, 12427–12431.
- (35) Fujimura, Y.; Jung, S.; Shirai, H. *Jpn. J. Appl. Phys.* **2001**, *40*, L1214–L1216.
- (36) Ma, Y.; Chen, X.; Pi, X.; Yang, D. *J. Phys. Chem. C* **2011**, *115*, 12822–12825.
- (37) Olivares-Amaya, R.; Amador-Bedolla, C.; Hachmann, J.; Atahan-Evrenk, S.; Sánchez-Carrera, R. S.; Vogt, L.; Aspuru-Guzik, A. *Environ. Sci.* [Online] **2011**, *4*, 4849 DOI: 10.1039/c1ee02056k
- (38) Kohn, W.; Becke, A. D.; Parr, R. G. *J. Phys. Chem.* **1996**, *100*, 12974–12980.
- (39) Hohenberg, P.; Kohn, W. *Phys. Rev.* **1964**, *136*, B864–B871.
- (40) Kohn, W.; Sham, L. *Phys. Rev.* **1965**, *140*, A1133–A1138.
- (41) Frisch, M. J.; et al. *Gaussian 09*, revision A.02; Gaussian, Inc.: Wallingford, CT, 2009.
- (42) Becke, A. D. *J. Chem. Phys.* **1993**, *45*, S648–S652.
- (43) (a) Perdew, J. P.; Wang, Y. *Phys. Rev.* **1992**, *45*, 13244–13249. (b) Perdew, J. P.; Burke, K.; Wang, Y. *Phys. Rev.* **1996**, *54*, 16533–16539. (c) Perdew, J. P. In *Electronic Structure of Solids*; Ziesche, P., Eschrig, H., Ed.; Akademie Verlag: Berlin, 1991; p 11.
- (44) (a) Krishnan, R.; Binkley, J. S.; Seeger, R.; Pople, J. A. *J. Chem. Phys.* **1980**, *72*, 650–654. (b) McLean, A. D.; Chandler, G. S. *J. Chem. Phys.* **1980**, *72*, 5639–5648. (c) Clark, T.; Chandrasekhar, J.; Spitznagel, G. W.; Schleyer, P. V. R. *J. Comput. Chem.* **1983**, *4*, 294–301.
- (45) Connolly, M. J. *Appl. Crystallogr.* **1983**, *16*, 548–558.
- (46) Vanderbilt, D. *Phys. Rev. B* **1990**, *41*, 7892–7895.
- (47) Clark, J. S.; Segall, M. D.; Pickard, C. J.; Hasnip, P. J.; Probert, M. I. J.; Refson, K.; Payne, M. C. *Z. Kristallogr.* **2005**, *220*, 567–570.
- (48) Accelrys Inc. *CASTEP Users Guide*; Accelrys Inc.: San Diego, CA, 2001.
- (49) Monkhorst, H. J.; Pack, J. D. *Phys. Rev. B* **1976**, *13*, 5188–5192.
- (50) Peng, X. H.; Ganti, S.; Alizadeh, A.; Sharma, P.; Kumar, S. K.; Nayak, S. K. *Phys. Rev.* **2006**, *74*, 035339(5 pages).
- (51) Hou, Z. F. *Condensed Matter* **2006**, arXiv:cond-mat/0607183v1, (accessed December 8, 2011).
- (52) Raniero, L.; Pereira, L.; Zhang, S.; Ferreira, I.; Águas, H.; Fortunato, E.; Martins, R. *J. Non-Cryst. Solids* **2004**, *338*, 206–210.
- (53) Gázquez, J. L.; Cedillo, A.; Vela, A. *J. Phys. Chem. A* **2007**, *111*, 1966–1970.
- (54) Cho, E.; Green, M. A.; Conibeer, G.; Song, D.; Cho, Y.; Scardera, G.; Huang, S.; Park, S.; Hao, X. J.; Huang, Y. et al. *Adv. Optoelectron.* [Online] **2007**, 69578; <http://www.hindawi.com/journals/aoe/2007/069578/abs/>, (accessed December 8, 2011).